Neutron diffraction, magnetostriction, and dielectric properties of orbitally ordered $FeCr_2S_4$ in external magnetic fields

J. Bertinshaw,[1,2] C. Ulrich,[1,2] A. Günther,[3] F. Schrettle,[3] M. Wohlauer,[3]
S. Krohns,[3] M. Reehuis,[4] A. Studer,[2] M. Avdeev,[2] D. V. Quach,[5]
J. R. Groza,[5] V. Tsurkan,[3,6] A. Loidl,[3] and J. Deisenhofer[3]

[1]*School of Physics, University of New South Wales, Sydney, NSW 2052, Australia*
[2]*Australian Nuclear Science and Technology Organisation, Lucas Heights, NSW 2234, Australia*
[3]*Experimental Physics V, Center for Electronic Correlations and Magnetism, University of Augsburg, D-86135 Augsburg, Germany*
[4]*Helmholtz-Zentrum Berlin für Materialien und Energie, D-14109 Berlin, Germany*
[5]*Department of Chemical Engineering and Materials Science, University of California, Davis, CA 95616, USA*
[6]*Institute of Applied Physics, Academy of Sciences of Moldova, MD-2028 Chisinau, Republic of Moldova*

(Dated: September 14, 2018)

Abstract

We report on neutron diffraction, thermal expansion, dielectric and specific heat measurements on polycrystalline $FeCr_2S_4$ samples in external magnetic fields. The ferrimagnetic and orbital ordering temperatures, $T_C \approx 170\,K$ and $T_{OO} \approx 10\,K$ are only weakly shifted in magnetic fields up to 9 T. The cubic lattice parameter is found to decrease when entering the orbitally ordered state below T_{OO}. This contraction does not significantly change in external fields up to 7.5 T. The magnetic moments of the Cr and Fe ions are reduced from the spin-only values throughout the magnetically ordered regime. The moments start to increase in the orbitally ordered regime when the magnetic fields become larger than 4.5 T and approach the expected spin-only values above about 5.5 T. Thermal expansion in magnetic fields and magnetostriction experiments indicate a contraction of the sample due to magnetic domains below about 60 K. In the orbitally ordered state this contraction is followed by a moderate expansion of the sample for fields larger than about 4.5 T, coinciding with the onset of the increase of the magnetic moments. The orbital ordering transition is accompanied by an anomaly in the dielectric constant. Below T_{OO} the dielectric constant depends on both the strength of the external magnetic field as well as the orientation of the external magnetic field with respect to the applied electric field.

PACS numbers: 61.05.fm, 71.70.Ej

I. INTRODUCTION

The interplay of orbital, lattice, and spin degrees of freedom is of fundamental importance in understanding the enormous variety of phenomena and ground states in transition-metal compounds.[1–3] In particular, the effects of short and long-range orbital ordering or of dynamic and static cooperative Jahn-Teller (JT) distortions on the magnetic ground state have been in the focus of condensed-matter physics throughout the research activities on, for example, cuprates and manganites. The respective JT active magnetic ions Cu^{2+} and Mn^{3+} usually exhibit a strong JT coupling in octahedral environment and contribute to cooperative JT distortions and orbital ordering far above room temperature, e.g. in $KCuF_3$ and $LaMnO_3$.[4–6] Similar electronic configurations are found in the case of compounds containing Fe^{2+} or Cr^{5+} ions in a tetrahedral crystal-field,[2,7–10] but the electron-lattice coupling is generally weaker and competes with spin-orbit coupling and exchange interactions, leading to strong fluctuations and frustration effects.

$FeCr_2S_4$ is a sulfur spinel that has been reported previously to exhibit a complex interplay of orbital correlations and magnetism, including ferrimagnetic ordering of the Cr and Fe sublattices below $T_C \approx 170\,K$[11,12] and long-range orbital order below $T_{OO} = 10$ K.[7,12–19] In addition, an anomaly in the low-field magnetization at $T_M = 60$ K revealed a change in the magnetic configuration,[12,20–25] which has recently been attributed to the formation of a non-collinear (possibly helical) spin configuration with an incommensurate modulation involving three different Fe sites as indicated by μSR and Mössbauer measurements.[26,27] The same temperature has also been associated with the onset of short-range orbital order (orbital liquid) and dynamic JT distortions, suggesting a mutual influence of spin configuration and orbital correlations.[12]

At room temperature $FeCr_2S_4$ crystallizes in the spinel structure with space group $Fd\bar{3}m$ with eight formula units per unit cell. The Cr^{3+} ions ($3d^3$, $S = 3/2$) occupy half of the octahedral sites and the Fe^{2+} ions ($3d^6$, $S = 2$) are at the centre of S^{2-} tetrahedron ions and form a diamond lattice of two interlacing FCC sublattices.[28] While the Cr sublattice is dominated by ferromagnetic exchange which is established through the 90° Cr–S–Cr bond, the exchange coupling within the Fe sublattice is rather weak and overruled by a much stronger antiferromagnetic coupling to the Cr ions, resulting in the ferrimagnetic arrangement. As the Cr^{3+} ions with a half-filled t_{2g} ground-state configuration do not possess orbital degrees

of freedom, the orbital physics in this compound is due to the orbital ground state of the Fe^{2+} ions. Because of the internal exchange field below T_C, the five-fold spin degeneracy of the lower-lying ^5E states is lifted and the level splits into five orbital doublets, of which the lowest is coupled to lattice vibrations and should lead to a dynamic JT effect and finally to a static cooperative JT distortion of the sulfur tetrahedra below $T = 10\,\mathrm{K}$.[28,29] Although the specific heat shows a λ-like anomaly at T_{OO}, an unambiguous signature of a structural JT distortion and a deviation from cubic symmetry remained evasive even in high-resolution structural studies. However, thermal expansion measurements have revealed a contraction of the lattice at T_{OO}.[12] Recently, the orbitally ordered state has been reported to exhibit a magnetic-field induced anomaly in the magnetization, showing the coupling of spin and orbital ordering in the system.[30]

In this study we focus on the influence of external magnetic fields on the structural, magnetic, and dielectric properties of $FeCr_2S_4$. In a detailed neutron diffraction study under applied magnetic fields, we microscopically identify changes in the cubic lattice parameter and the magnetic moments of Cr and Fe ions using a collinear ferrimagnetic model. Combining these results with specific heat, thermal expansion and dielectric measurements in applied magnetic fields, we propose a modified $B - T$ phase diagram of $FeCr_2S_4$.

II. EXPERIMENTAL DETAILS

Polycrystalline samples of $FeCr_2S_4$ for neutron experiments were prepared by solid-state reaction using high-purity elements. Post growth annealing under a chalcogen atmosphere was performed to achieve a pure stoichiometric ratio, which has been shown previously to exhibit the strongest low temperature anomaly.[12] For preparation of dense samples for thermal expansion and specific heat measurement, we used a spark-plasma-sintering (SPS) technique as described in Ref. 12. While both samples exhibit the orbital ordering transition at about 10 K, the sample obtained by SPS showed a reduced ferrimagnetic transition temperature of 165 K in comparison to the one used for the neutron diffraction study with $T_C = 180\,\mathrm{K}$. Thermal-expansion, magnetostriction and dielectric experiments were carried out in a home-built setup using a capacitance bridge (AH 2700 Hagerling) for temperatures from 1.5-300 K and in external magnetic fields up to 14 T. The sample had the shape of a platelet and the expansion was measured along the direction of the applied magnetic field,

which is perpendicular to the platelet. Dielectric measurements were perfomed using silver-paint contacts applied on both sides of the platelike sample, the magnetic field was applied perpendicular and parallel to the electric field. The heat capacity was measured in a physical properties measurements system (PPMS, Quantum Design) for temperatures between 1.8 K and room temperature and in external magnetic fields up to 9 T.

High resolution powder neutron diffraction measurements were performed using the instrument Echidna, located at the Bragg Institute, ANSTO, Sydney, Australia. Echidna is equipped with 128 ^{3}He linear position sensitive detectors that are scanned in position to produce high resolution diffraction patterns. A Ge monochromator was aligned on the (331) reflection with a take-off angle of 140° to select a wavelength of 2.4395 Å with a calculated accessible Q-range of 0.2-5.1 Å^{-1}. Collimation ensured a minimum FWHM resolution of ∼0.4°. To achieve a good signal to noise ratio, each diffraction pattern was collected for 6 hours with an angular step of 0.05°. The symmetry of the $FeCr_2S_4$ crystal and magnetic structures were characterized by performing a least-squares Rietveld refinement of the powder neutron diffraction data, using the FULLPROF software suite.[31]

The high-intensity powder neutron diffractometer Wombat, located at the Bragg Institute, was used to conduct temperature and applied magnetic field dependency studies of the magnetic and crystal structures of $FeCr_2S_4$. Magnetic fields up to 7.5 T were applied using a vertical closed-cycle cryomagnet (Cryogenic Ltd.). Wombat uses a monolithic position-sensitive ^{3}He detector, enabling fast collection times with little penalty to resolution. A vertically focused Ge monochromator was set to align on the (113) reflection, with a 90° take-off angle, giving an incident wavelength of 2.41 Å and an accessible Q-range of 0.5-4.9 Å^{-1}. No collimation was used to maximize the count rate, resulting in a required 10 minute collection time per scan.

III. RESULTS AND DISCUSSION

A. Specific Heat

In Fig. 1 we compare the temperature dependence of the specific heat in the representation C_P/T vs. T in zero and 9 T fields. While the sharp anomaly at the ferrimagnetic transition at 165 K in zero field is strongly broadened at 9 T, the changes of the λ-like anomaly around

10 K at the orbital-ordering transition (shown in the inset for several external magnetic fields) exhibits only a small shift and a transfer of associated entropy to higher temperatures with increasing magnetic field. This indicates that the orbitally ordered phase is rather stable with respect to the applied magnetic field, but critical fluctuations are favored to occur at higher temperatures already. A shift of the anomaly and an entropy transfer in 14 T has been reported, which is similar to the one we observe in 9 T.[32]

The temperatures of the orbital-ordering transition at 9.2, 9.5, 9.9, and 10.3 K for 0, 1, 6, and 9 T, respectively, were evaluated from the C_P/T dependencies in terms of the temperatures where the data starts to deviate from a linear fit at temperatures above the maximum (see inset of Fig. 1). The ferrimagnetic transition temperature in zero-field is determined by the same procedure as $T_C = 165$ K. In 9 T the transition temperature has been evaluated as the intersection point of two linear extrapolations below and above the broad maximum (see Fig. 1).

The influence of an external magnetic field on the magnetization of $FeCr_2S_4$ in the orbitally ordered phase was reported recently and it was proposed that there exists a new magnetic phase for fields larger than 5.5 T, which might be related to the restoration of a commensurate collinear spin structure.[30] As reported earlier the orbital-ordering transition is accompanied by a contraction of the lattice revealed by thermal expansion measurements.[12]

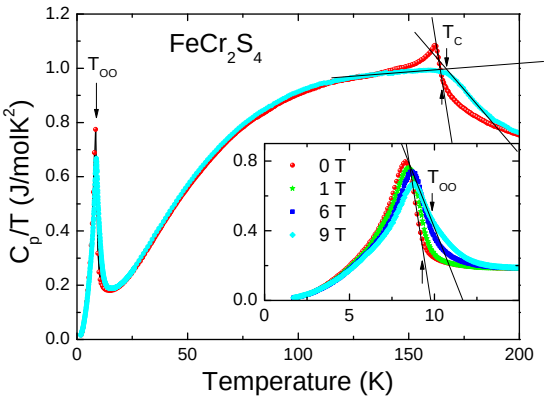

FIG. 1. (Color online) Temperature dependency of the specific-heat in zero and 9 T plotted as C_P/T vs. T showing the ferrimagnetic and orbital ordering transitions at T_C and T_{OO}, respectively. Inset: Changes of the anomaly at the orbital-ordering transition for 0, 1, 6, and 9 T. Solid lines indicate linear fits to estimate the transition temperatures as described in the text.

Therefore, we performed a detailed neutron diffraction study to search for possible indications of a symmetry-lowering and microscopic evidence for the contraction, which will be discussed in the following.

B. Neutron Diffraction

High resolution neutron diffraction patterns were collected at T = 4 K, 15 K, 70 K, and 100 K. Between 15 K and 4 K, the experimental data does not demonstrate the emergence of additional peaks in the diffraction signal, which would directly reveal a reduction in symmetry corresponding to the transition to a cooperative JT state. In this state stabilized long-range order of the structurally distorted S-tetrahedra is likely to manifest as a transition from a cubic to tetragonal spinel structure.[1] However, as the maximum displacement of the ligand S^{2-} ions has been estimated to be ∼0.04 Å, the resulting splitting of the cubic Bragg reflections might be well below the resolution limit of the available neutron diffraction instrumentation,[7] and indeed such splitting could not be resolved in our data. Instead, a careful treatment of the Rietveld least squares refinement was applied to reveal the subtle temperature induced changes in lattice parameter and Fe and Cr ion magnetic moments.

Figure 2 presents the result of the Rietveld refinement of the 4 K dataset. Refinements of the diffraction patterns were performed in the high-symmetric cubic spinel structure with the

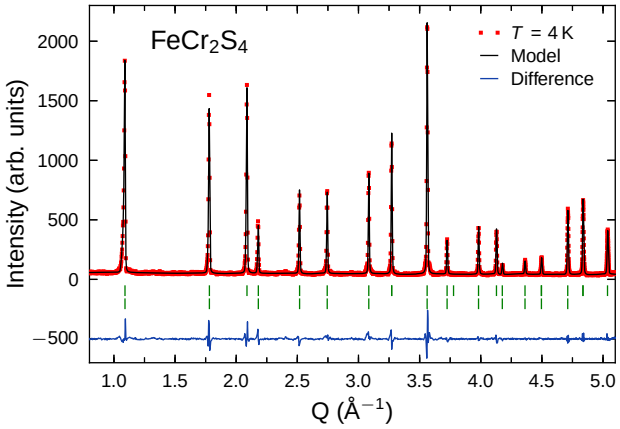

FIG. 2. (Color online) Neutron powder diffraction conducted at 4 K. Rietveld refinement has been performed to fit the pattern to the cubic spinel structural model. The magnetic structure is defined as antiparallel alignment of the Fe and Cr spins collinear along the crystal axes.

TABLE I. Results of the crystal structure refinements of $FeCr_2S_4$ from neutron powder diffraction ($\lambda = 2.4395$ Å). The structure refinements of the data sets collected at 4 and 15 K were carried out in the cubic space group $Fd\bar{3}m$. The nuclear and magnetic residuals are defined as $R_N = \sum ||F_{obs}| - |F_{cal}|| / \sum |F_{obs}|$ and $R_M = \sum ||I_{obs}| - |I_{cal}|| / \sum |I_{obs}|$, respectively.

Temperature	4 K	15 K
$a = b = c$ [Å]	9.97989(3)	9.98018(3)
μ(Fe) [μ_B]	–3.69(6)	–3.72(7)
μ(Cr) [μ_B]	2.64(3)	2.63(3)
x(S)	0.2585(3)	0.2586(3)
R_N	2.63	2.30
R_M	4.68	4.39

space group $Fd\bar{3}m$ (no. 227). The atoms are located at the following Wyckoff positions: Fe at 8a ($\frac{1}{8}$, $\frac{1}{8}$, $\frac{1}{8}$), Cr at 16d ($\frac{1}{2}$, $\frac{1}{2}$, $\frac{1}{2}$), and S at 32e (x, x, x). The magnetic phase symmetry was defined to align the Fe and Cr moments antiparallel along the structural c-direction as our data indicates that the spins are aligned along the cubic crystal axes. There is no evidence for a weak spin canting within the experimental resolution. Instrumental parameters were fitted using the diffraction pattern measured at 4 K, and fixed for the refinement of the succeeding datasets. Fitted structural parameters of the Rietveld refinements for for 4 K and 15 K are listed in Table I. No significant insight could be gained from the sulfur position parameter x within the resolution limits of the instrument. Notable is a deviation in the trend of the cubic lattice parameter, outside of the calculated error, evident between $T = 4$ K and 15 K, shown in the inset of Fig. 4(a).

To investigate the nature of this distortion and other potential subtle deviations, the crystal and magnetic structures were further investigated in a thorough neutron diffraction temperature dependency study. Diffraction patterns were collected on the high intensity Wombat instrument at temperatures from 4 K to 200 K in 1 K steps, then 202 K to 300 K in 2 K steps. The results have been plotted as a heat-map in Fig. 3, which reveals the transition to ferrimagnetic order below $T_C \approx 180$ K. A logarithmic color scale has been used to enhance

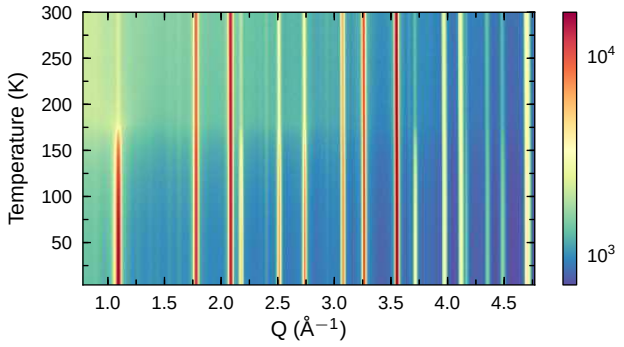

FIG. 3. (Color online) Neutron diffraction data from 4 K up to 300 K represented in a contour plot with a logscale color map to enhance subtle modifications, revealing $T_{\mathrm{C}} \approx 180\,\mathrm{K}$.

subtle changes in the diffraction signal, such as the increased background at lower-Q caused by short-range spin correlations above the transition to ferrimagnetic order. As with the high-resolution diffraction data, no peak splitting is visible down to lowest temperatures.

The full 4 K to 300 K diffraction dataset was systematically refined to the cubic spinel space group $Fd\bar{3}m$. Initial crystal and magnetic phase parameters were set using the results of the refinement of the high-resolution data. Instrumental characteristics such as peak shape parameters were fitted for the 4 K dataset and fixed for succeeding temperature refinements. The refined cubic lattice parameter and magnetic moments of the Cr and Fe ions are plotted in Fig. 4(a) and 4(b), respectively, demonstrating the consistency between the temperature-dependency and high-resolution neutron diffraction studies. The insert of Fig. 4(a) reveals a distinct reduction of the cubic lattice parameter at 10 K. Such a contraction is indicative of an antiferrodistortive tetragonal modification of the cubic symmetry and strong microscopic indication of the transition to a long range orbital order below $T_{\mathrm{OO}} = 10\,\mathrm{K}$. This result compares well with our specific heat study and previous bulk thermal expansion results.[12]

In Fig. 4(a) we show that the temperature-dependent trend in the lattice parameter from T_{C} to 60 K is well described by normal anharmonic solid lattice dynamics, fit accordingly to $V(\mathrm{T}) = V_O[1 + A/[\exp(\theta/\mathrm{T}) - 1]]$, where V_O represents the cell volume extrapolated to 0 K, θ is an averaged Debye temperature, and A is a fitting constant. More intriguing is a deviation from the fitted curve for a normal anharmonic solid below 60 K, which indicates enhanced shrinking of the lattice parameter. This result is consistent with previous bulk thermal expansion measurements,[12] which has previously been associated with short-range orbital fluctuations below $T_{\mathrm{S}} \approx 60\,\mathrm{K}$[12] and the emergence of a non-collinear spin configuration.[26]

We found no direct evidence of a deviation from a simple collinear magnetic structure, within the resolution limits of the neutron diffraction technique. The temperature dependency of the magnetic moment of the Fe and Cr ions as determined from the refinement of the neutron diffraction data are presented in Fig. 4(b). The respective values of –3.69 μ_B and 2.64 μ_B at 4 K are consistent with values recently determined in a neutron diffraction study,[18] along with other experimental and theoretical approaches, which are compared in Table II. In particular, density-functional based calculations found reduced spin moments of –3.3 μ_B and 2.7 μ_B for both types of ions and an orbital moment of –0.13 μ_B on the Fe ions,[36,37] which are in agreement with our resulting total magnetic moments within experimental error. The orbital contribution of the Fe ions is argued to originate from spin-orbit coupling,[37] which is in agreement with the single-ion picture, where the second-order con-

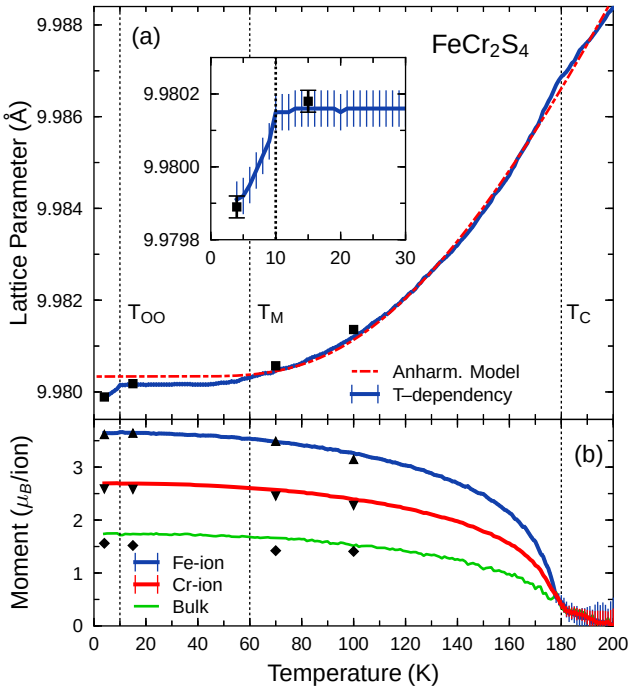

FIG. 4. (Color online) (a) Temperature dependency of the refined cubic lattice parameter. The dashed line corresponds to the behavior of a normal anharmonic solid, from which $FeCr_2S_4$ deviates due to short range orbital order at $T_S \approx 60\,K$. Inset: At $T_{OO} = 10\,K$, the anomaly in lattice parameter is a result of antiferrodistortive distortion of the lattice with the onset of long range orbital order. (b) Temperature dependency of the magnetic moment parameter of the Fe and Cr ions.

TABLE II. Comparison of the derived magnetic moments of the Fe and Cr ions and the total magnetic moment per formula unit (in units of the Bohr magneton μ_B) from neutron diffraction (ND), x-ray spectroscopy (XPS), magnetization measurements (Mag.), and theoretical approaches (Calc.) for lowest temperatures.

	This Work	ND[18]	ND[11]	XPS[33]	Mag.[34]	Mag.[21]	Mag.[30]	Calc.[35]	Calc.[36]
Fe^{2+}	−3.69	−3.52	−4.2	−3.89	-	-	-	−3.70	−3.40
Cr^{3+}	2.64	2.72	2.9	2.71	-	-	-	3.11	2.66
Total/f.u.	1.59	1.92	1.6	1.53	1.52	1.84	1.6	2.0	1.92

tribution of spin-orbit coupling yields an effective g-factor $g = 2.1$.[38] However, the spin-only moments are reduced from –4.2 μ_B for Fe^{2+} with $S = 2$ and $g = 2.1$ and 3.0 μ_B for Cr^{3+} with spin $S = 3/2$ and $g = 2$.

Recent reports have indicated modifications to exhibited magnetic properties of $FeCr_2S_4$ under large applied magnetic fields.[30,32] We have performed neutron diffraction experiments under applied magnetic fields in order to reveal potential deviations in the crystallographic and magnetic structures. We have studied deviations in the refined lattice and magnetic moment parameters of the Fe^{2+} and Cr^{3+} ions under external applied magnetic fields of up to 7.5 T. Neutron diffraction patterns were collected on the instrument Wombat at ANSTO under applied magnetic fields from 3 T up to 7.5 T in 0.5 T steps at temperatures from 5 K up to 15 K in 1 K steps. For the Rietveld refinements, the collected diffraction patterns were treated using the cubic spinel structure and collinear antiparallel magnetic structure as determined previously. Crystal and magnetic structural parameters were initially set based upon the results of the zero-field refinement results. Under an initial relatively small applied field, the Fe- and Cr-ion spins structure of cubic $FeCr_2S_4$ preferentially rotates to align along the crystal axis in the applied magnetic field direction. Additional parameters to account for this preferential orientation of the magnetic phase were implemented in the refinement in order to obtain an acceptable fit.

The results of the study are presented in Fig. 5. In Fig. 5(a) the observed reduction of the cubic lattice parameter below T_{OO} in zero field remains visible under applied magnetic fields up to 7.5 T, confirming that the transition to an orbitally ordered cooperative JT state

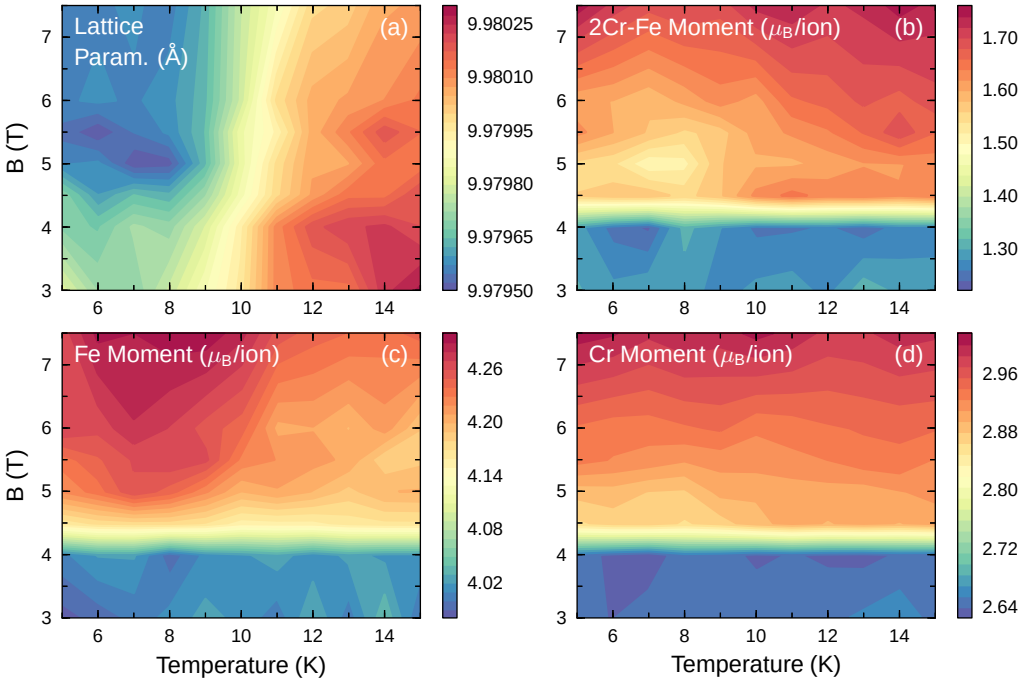

FIG. 5. (Color online) Results of the magnetic field dependency study have been plotted as contour maps. (a) The cubic lattice parameter shows a clear contraction at T= 10 K for all magnetic fields studied. The refined (b) bulk magnetic moment, (c) Fe-ion moment and (d) Cr-ion moment parameters reveal a clear increase at around 4.5 T, which is interpreted as the realization of full spin-only values under an applied magnetic field of the order of the anisotropy field, as described in the text.

remains stable with respect to even relatively large external magnetic fields.

A clear increase in the obtained magnetic moment of the Fe^{2+} and Cr^{3+} ions occurs at around 4.5 T (Fig. 5b,c,d), with spin-only values of –4.2μ_B and 3.0μ_B approached for fields above 5.5 T, respectively. The reduced magnetic moments observed in neutron diffraction in zero-field suggest the existence of a transverse quasi-paramagnetic component of the magnetic moments for both ions throughout the magnetically ordered regime $T < T_C$. When a magnetic field of the order of the anisotropy field is applied,[39] these transverse components are suppressed and the magnetic moments derived from neutron diffraction data reach the full spin-only values of the longitudinal magnetization. This implies that the transverse components in zero-field are stabilized by the magneto-crystalline anisotropy originating from spin-orbit coupling effects.

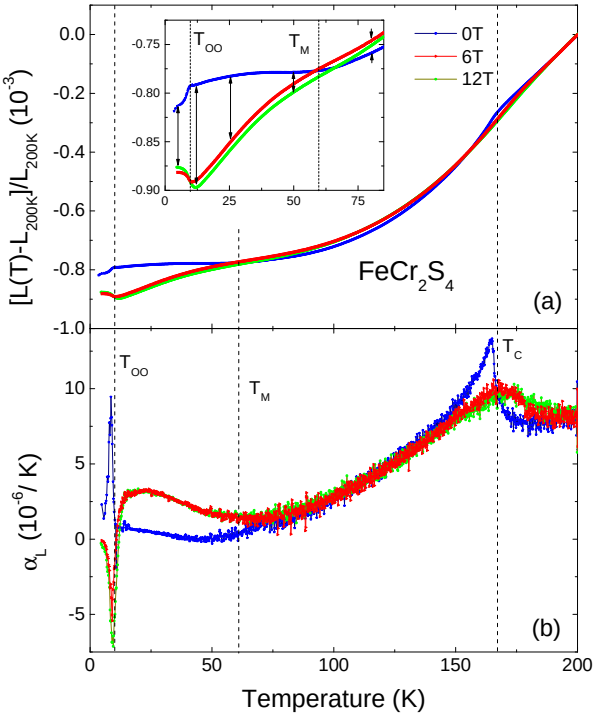

FIG. 6. (Color online) Temperature dependency of (a) the thermal expansion normalized to the value at 200 K and (b) the thermal expansion coefficient α in magnetic fields of 0, 6, and 12 T. Inset: thermal expansion for $T \leq 80$ K on an enlarged scale. Arrows indicate selected temperatures where the differences in the thermal expansion in constant magnetic fields are compared to the magnetostriction results at constant temperature (see Fig. 7)

C. Thermal Expansion and Magnetostriction

The temperature dependencies of the thermal expansion in applied magnetic fields of a dense polycrystalline sample (spark-plasma sintering) are shown in Fig. 6(a) together with zero-field data reported in Ref. 12. In the paramagnetic phase at 200 K we do not expect any significant magneto-strictive effects enabling us to compare directly the effect of the external magnetic field, by normalizing the data to the value $L(200\,\mathrm{K})$. The temperature dependence of the thermal expansion in zero field (previously published in Ref. 12) clearly shows a contraction of the lattice upon entering the orbitally ordered regime at 10 K, which

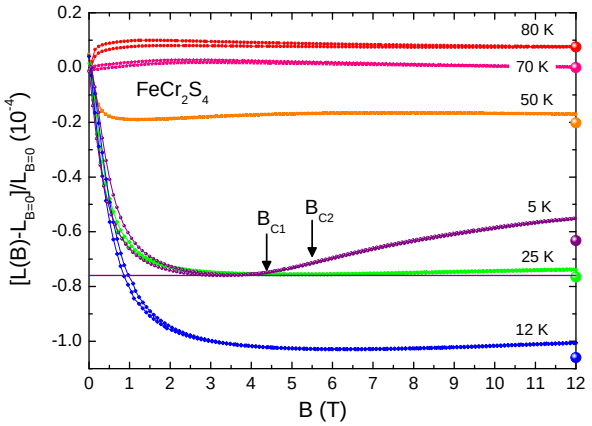

FIG. 7. (Color online) Thermal expansion vs. magnetic field normalized to the zero-field value measured at different temperatures. The large spheres indicate the values derived from the temperature dependencies as described in the text. The arrow at B_{c1} marks the field where the sample starts to expand again along the direction of the magnetic field.

is in agreement with the temperature evolution of the lattice parameter in Fig. 4 determined by the neutron diffraction experiment.

The effect of the external magnetic field is barely visible above 100 K, but in agreement with the specific-heat data a clear broadening of the anomaly at the ferrimagnetic transition is found in the linear thermal-expansion coefficient $\alpha_L = 1/L(\partial L/\partial T)$ for the direction parallel to the applied magnetic field (Fig. 6(b)). In the temperature range $60 \leq T \leq 130$ K only slight deviations from the zero-field curve can be detected. However, below about 60 K the sample contracts much stronger when a magnetic field is applied. This temperature coincides with the temperature T_{M} where a transition from a collinear to a non-collinear spin configuration with three different Fe sites has been reported by μSR and where orbital fluctuations and a dynamic JT distortion set in.[12,26,27] The relative change of the thermal expansion upon entering the orbitally ordered phase below 10 K is similar to the zero-field data, but under applied fields of 6 T and 12 T the sample expands again towards lowest temperatures, which is clearly seen in the negative thermal expansion coefficient for the transition in magnetic fields. The temperatures of the minima in the thermal expansion in magnetic fields are used as a measure of the orbital-ordering transition temperatures.

To get additional insight in the influence of the magnetic field on the thermal expansion we measured the magnetostriction effect at different temperatures. The corresponding data

is shown in Fig. 7 for selected temperatures, which are also indicated by arrows in the inset of Fig. 6(a). The values at 12 T are compared with the values (large solid symbols in Fig. 7) obtained by subtracting the corresponding temperature dependencies in Fig. 6(a). The different data sets agree well, the deviations at lower temperatures might indicate small variations in temperature during the different measurements. At high temperatures the field effects are small and the almost field independent zero-magnetostriction curve at 70 K indicates a sign change as expected from the temperature dependence of the thermal expansion. Accordingly, the largest contraction is observed at 12 K, just above the orbital ordering transition. At both 12 K and 25 K the lattice contracts strongest in field from zero to about 2 T, undergoes a very broad shallow minimum, and tends to saturate up to the highest measured fields. In the orbitally ordered state a broad but clear minimum develops at around 3-4 T, signaling the change from a contraction to an expansion of the sample in higher magnetic fields. The external fields B_{c1} and B_{c2} associated with this change are estimated by the values where the magnetostriction curve increases visibly from the minimal value (indicated as a constant solid line)and by the inflection points, respectively.

From the neutron scattering results in magnetic field, it is clear that the volume contraction of the lattice below T_{OO} is still present in magnetic fields up to 7.5 T. The strong effects seen in the macroscopic thermal expansion measurement of the polycrystalline SPS sample must therefore be related to the existence of magnetic domains in the investigated sample. In fact, the largest changes occur in fields smaller than 2 T (see Fig. 7) at temperatures below $T_{\mathrm{M}} = 60$ K, which has previously been reported to correspond with a transition from a collinear to an incommensurate magnetic structure.[26] This phase was shown to exhibit strong domain formation,[22] and small hysterical effects are visible in the data. Within the magnetic field range of our study, the contraction of the sample seems to saturate above 3-4 T and above T_{OO}, indicating that the magnetic domain structure has been stabilized. In the orbitally ordered state, however, an expansion of the sample sets in between B_{c1} and B_{c2}. We suppose that any further changes are a result of changes of the magnetic anisotropy, which comes into play once an almost single-domain state has been formed.

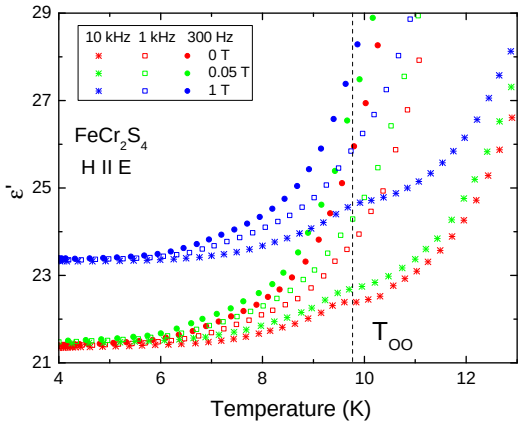

FIG. 8. (Color online) Temperature dependence of the dielectric constant ϵ' in polycrystalline $FeCr_2S_4$ for selected frequencies. The measurement were performed in zero-magnetic field and with applied external magnetic field (0.05 T and 1 T) parallel to the direction of the electrical field.

D. Dielectric Spectroscopy

The possible occurrence of multiferroicity in the orbitally ordered phase of $FeCr_2S_4$ has been put forward recently.[40] The temperature dependence of the dielectric constant ϵ' in magnetic fields (oriented parallel to the electric field, $\mathbf{H} \parallel \mathbf{E}$) up to 1 T is shown for selected frequencies in Fig. 8). Here, we focus on dielectric properties in a restricted temperature regime below 13 K. For all investigated frequencies and all magnetic fields ϵ' decreases with decreasing temperature and becomes almost temperature independent below 6 K in the orbitally ordered state. An anomaly at T_{OO} is visible for all magnetic fields in the curves measured at 10 kHz. For lower frequencies the transition is masked by the strong increase towards higher temperatures, which is assigned to relaxation processes described previously in single crystalline samples Ref.19. Here, we want to focus on the clear increase of the dielectric constant in magnetic field between 0.05 and 1 T. Therefore, we have investigated the field dependence of the dielectric constant with the magnetic field applied parallel ($\mathbf{H} \parallel \mathbf{E}$) and perpendicular to the electric field ($\mathbf{H} \perp \mathbf{E}$). We chose a temperature of 5 K, where the dielectric constant depends only on the magnetic field. The results are plotted in figure 9. In agreement with the data in Fig. 8 ϵ' increases with increasing magnetic field for $\mathbf{H} \parallel \mathbf{E}$. The largest changes take place in magnetic fields up to about 0.5 T, and also hysterical

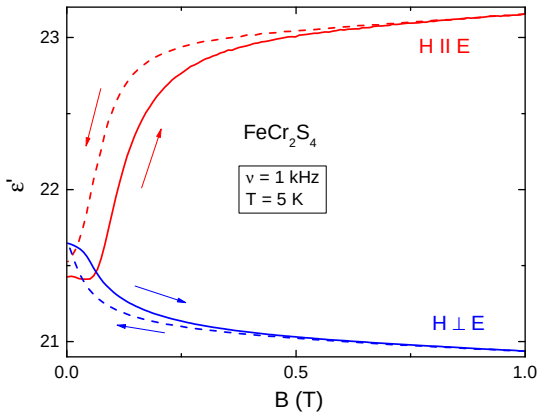

FIG. 9. (Color online) Magnetic field dependence of the dielectric constant ϵ' in polycrystalline $FeCr_2S_4$ for $\nu = 1\,\mathrm{kHz}$ and at $T = 5\,\mathrm{K}$. The blue lines are the results of $\epsilon'(H)$, electrical field parallel to the magnetic field, the red lines denote the measurement with electrical field perpendicular to the magnetic field. The arrows show the measurements with increasing (solid lines) and decreasing (dashed lines) magnetic fields.

effects are present below this value. By contrast, the dielectric constant decreases with increasing magnetic field for $\mathbf{H} \perp \mathbf{E}$, again showing the largest changes and a hysteresis below fields of 0.5 T.

The observed anomalies in the dielectric constant at T_{OO} may indicate a ferroelectric transition as claimed in Ref. 40 or be the result of magnetoelectric coupling. While unambiguous measurements of an intrinsic ferroelectric polarization are difficult to perform in $FeCr_2S_4$, the magnetic-field dependence of the dielectric constant supports the existence of magnetoelectric coupling. The increase and the hysteretic effects below 0.5 T for $\mathbf{H} \parallel \mathbf{E}$ are similar to the reorientation effects of magnetic domains in low-magnetic fields[22] and suggest a coupling of magnetic and dielectric domains. Together with the decrease of ϵ' for $\mathbf{H} \perp \mathbf{E}$ this may point to a contribution to the dielectric constant $\Delta\epsilon'(\mathbf{M}, \sphericalangle(\mathbf{M}, \mathbf{E}))$ which depends on the magnetization $\mathbf{M}$ of the sample and the angle of $\mathbf{M}$ with respect to the applied electric field $\mathbf{E}$.

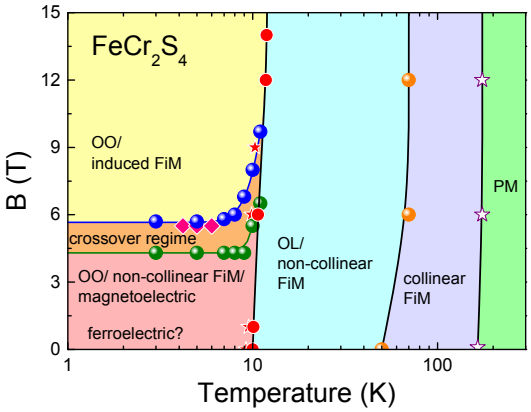

FIG. 10. (Color online) $B-T$ phase diagram of $FeCr_2S_4$(logarithmic temperature scale). OO: orbital order, FiM: ferrimagnet, OL: orbital liquid, PM: paramagnet. Values were taken from the respective temperature and field dependences of the thermal expansion and magnetostriction $\Delta L(B,T)$ (spheres) and the specific heat $C_P(T,B)$ (stars). Values from the magnetization $M(T,B)$ (diamonds) were taken from Refs. 30. Lines are to guide the eyes.

IV. CONCLUSIONS

Our results are summarized in a modified $B-T$ phase diagram shown in Fig. 10. We plotted the orbital- and magnetic ordering and temperatures determined from the specific heat and thermal expansion measurements. The temperatures where the magnetic transition and short-range orbital order were observed in magnetization measurements and the ones, where the thermal expansion curves measured in 6 T and 12 T intersect with the one measured in zero field, were also added to the phase diagram. The estimates for the fields B_{c1} and B_{c2} yield the boundaries of a *crossover region* for $T < T_{OO}$. B_{c2} is in good agreement with the values of the change of the magnetization reported by Ito et al.[30]. This region coincides with the magnetic-field induced increase of the magnetic moments of the Fe and Cr ions observed by neutron diffraction as discussed above. Therefore we assign the region for $B > B_{c2}$ and $T < T_{OO}$ to an *induced ferrimagnetic state*, which is characterized by the expected spin-only moments of Fe and Cr. The fields B_{c1} and B_{c2} correspond to the order of magnitude of the fields to overcome the magnetocrystalline anisotropy. Therefore, we conclude that the transverse components of the magnetization are related to the magnetocrystalline anisotropy via spin-orbit coupling.

Whether the corresponding magnetic structure is collinear or not could not be determined from the neutron diffraction data. Muon spin rotation and Mössbauer investigations as a function of magnetic field may be able to answer this question. We find evidence for a magnetoelectric effect in the orbitally ordered state, which depends on the relative orientation of the applied magnetic and electric fields. The possible existence of a ferroelectric state below T_{OO} can not be confirmed by our data.

ACKNOWLEDGMENTS

We thank K.-H. Höck, H.-A. Krug von Nidda, B. Lake, M. Schmidt, and Z. Wang for fruitful discussions and A. Schmidt for technical assistance. We acknowledge partial support by the Deutsche Forschungsgemeinschaft via TRR 80 (Augsburg-Munich). M. W. and S. K. acknowledge the support by the Federal Ministry of Education and Research via project 03EK3015. J. B. and C. U. acknowledge the support of the Australian Research Council through the Discovery Projects funding scheme (project DP110105346).

[1] K. I. Kugel and D. I. Khomskii, Phys. Usp. **136**, 621 (1982).

[2] L. F. Feiner, J. Phys. C: Solid State Phys. **15**, 1495 (1982).

[3] Y. Tokura and N. Nagaosa, Science **288**, 462 (2000).

[4] S. Kadota, I. Yamada, S. Yoneyama, and K. Hirakawa, J. Phys. Soc. Jpn. **23**, 751 (1967).

[5] L. Paolasini, R. Caciuffo, A. Sollier, P. Ghigna, and M. Altarelli, Phys. Rev. Lett. **88**, 106403 (2002).

[6] Y. Murakami, J. P. Hill, D. Gibbs, M. Blume, I. Koyama, M. Tanaka, H. Kawata, T. Arima, Y. Tokura, K. Hirota, and Y. Endoh, Phys. Rev. Lett. **81**, 582 (1998).

[7] L. F. Feiner, J. Phys. C: Solid State Phys. **15**, 1515 (1982).

[8] Z. Wang, M. Schmidt, A. Günther, S. Schaile, N. Pascher, F. Mayr, Y. Goncharov, D. L. Quintero-Castro, A. T. M. N. Islam, B. Lake, H.-A. Krug von Nidda, A. Loidl, and J. Deisenhofer, Phys. Rev. B **83**, 201102 (2011).

[9] D. Wulferding, P. Lemmens, K.-Y. Choi, V. Gnezdilov, Y. G. Pashkevich, J. Deisenhofer, D. Quintero-Castro, A. T. M. NazmulIslam, and B. Lake, Phys. Rev. B **84**, 064419 (2011).

[10] Z. Wang, M. Schmidt, A. Gunther, F. Mayr, Y. Wan, S. H. Lee, H. Ueda, Y. Ueda, A. Loidl, and J. Deisenhofer, Phys. Rev. B **85**, 224304 (2012).

[11] G. Shirane, D. E. Cox, and S. J. Pickart, J. Appl. Phys. **35**, 954 (1964).

[12] V. Tsurkan, O. Zaharko, F. Schrettle, C. Kant, J. Deisenhofer, H.-A. Krug von Nidda, V. Felea, P. Lemmens, J. R. Groza, D. V. Quach, F. Gozzo, and A. Loidl, Phys. Rev. B **81**, 184426 (2010).

[13] R. Englman and B. Halperin, Phys. Rev. B **2**, 75 (1970).

[14] M. Spender and A. Morrish, Solid State Commun. **11**, 1417 (1972).

[15] L. Brossard, J. Dormann, L. Goldstein, P. Gibart, and P. Renaudin, Phys. Rev. B **20**, 2933 (1979).

[16] M. Eibschutz, S. Shtrikman, and Y. Tenenbaum, Phys. Lett. A **24**, 563 (1967).

[17] G. Hoy and K. Singh, Phys. Rev. **172**, 514 (1968).

[18] S. J. Kim, W. C. Kim, and C. S. Kim, J. Appl. Phys. **91**, 7935 (2002).

[19] R. Fichtl, V. Tsurkan, P. Lunkenheimer, J. Hemberger, V. Fritsch, H.-A. Krug von Nidda, E.-W. Scheidt, and A. Loidl, Phys. Rev. Lett. **94**, 027601 (2005).

[20] V. Tsurkan, M. Lohmann, H.-A. Krug von Nidda, A. Loidl, S. Horn, and R. Tidecks, Phys. Rev. B **63**, 125209 (2001).

[21] V. Tsurkan, M. Baran, R. Szymczak, H. Szymczak, and R. Tidecks, Physica B **296**, 301 (2001).

[22] V. Tsurkan, J. Hemberger, M. Klemm, S. Klimm, A. Loidl, S. Horn, and R. Tidecks, J. Appl. Phys. **90**, 4639 (2001).

[23] D. Maurer, V. Tsurkan, S. Horn, and R. Tidecks, J. Appl. Phys. **93**, 9173 (2003).

[24] M. Mertinat, V. Tsurkan, D. Samusi, R. Tidecks, and F. Haider, Phys. Rev. B **71**, 100408 (2005).

[25] C. Shen, Z. Yang, R. Tong, G. Li, B. Wang, Y. Sun, and Y. Zhang, J. Magn. Magn. Mater. **321**, 3090 (2009).

[26] G. M. Kalvius, A. Krimmel, O. Hartmann, R. Wäppling, F. E. Wagner, F. J. Litterst, V. Tsurkan, and A. Loidl, J. Phys.: Condens. Matter **22**, 052205 (2010).

[27] J. Engelke, F. Litterst, A. Krimmel, A. Loidl, F. Wagner, G. Kalvius, and V. Tsurkan, Hyperfine Interact. **202**, 57 (2011).

[28] J. B. Goodenough, J. Phys. Chem. Solids **25**, 151 (1964).

[29] G. A. Gehring and K. A. Gehring, Rep. Prog. Phys. **38**, 1 (1975).

[30] M. Ito, Y. Nagi, N. Kado, S. Urakawa, T. Ogawa, A. Kondo, K. Koyama, K. Watanabe, and K. Kindo, J. Magn. Magn. Mater. **323**, 3290 (2011).

[31] J. Rodrguez-Carvajal, Physica B **192**, 55 (1993).

[32] C. Shen, Z. Yang, R. Tong, Z. Zi, W. Song, Y. Sun, L. Pi, and Y. Zhang, J. Appl. Phys. **109**, 07E144 (2011).

[33] E. Z. Kurmaev, A. V. Postnikov, H. M. Palmer, C. Greaves, S. Bartkowski, V. Tsurkan, M. Demeter, D. Hartmann, M. Neumann, D. A. Zatsepin, V. R. Galakhov, S. N. Shamin, and V. Trofimova, J. Phys.: Condens. Matter **12**, 5411 (2000).

[34] V. Zestrea, V. Y. Kodash, V. Felea, P. Petrenco, D. V. Quach, J. R. Groza, and V. Tsurkan, J. Mater. Sci. **43**, 660 (2008).

[35] M. S. Park, S. K. Kwon, S. J. Youn, and B. I. Min, Phys. Rev. B **59**, 10018 (1999).

[36] S. Sarkar, T. Maitra, R. Valenti, and T. Saha-Dasgupta, Phys. Rev. B **82**, 041105 (2010).

[37] S. Sarkar, M. De Raychaudhury, I. Dasgupta, and T. Saha-Dasgupta, Phys. Rev. B **80**, 201101 (2009).

[38] P. Gibart, J. Dormann, and Y. Pellerin, Phys. Status Solidi **36**, 187 (1969).

[39] T. Ogasawara, K. Ohgushi, H. Okamoto, and Y. Tokura, J. Phys. Soc. Jap. **75**, 083707 (2006).

[40] L. Lin, D. Liu, Z. Zhao, J. Wen, Z. Yan, S. Dong, and J. Liu, in *http://meetings.aps.org/link/BAPS.2013.MAR.F21.1* (2013).